

SULFIDE-OXIDE MINERAL ASSEMBLAGES AS INDICATOR OF SULFUR AND OXYGEN REGIME IN MODERN SUBMARINE MASSIVE SULFIDE DEPOSITS

Nadezhda N. Mozgova
IRAS Institute of Geology of Ore Deposits, Mineralogy, Petrology, and Geochemistry RAS, Moscow, Russia
mozgova@igem.ru

Yury S. Borodaev
Moscow State University, Moscow, Russia

Tamara V. Stepanova, Georgiy A. Cherkashev
All-Russia Research Institute for Geology and Mineral Resources of the World Ocean

Tatyana Yu. Uspenskaya
IRAS Institute of Oceanology RAS, Moscow

During ore-forming hydrothermal processes at the oceanic bottom, the behavior of sulfur and oxygen varies like at the continents. These variations are illustrated by the sulfide-oxide mineral assemblages from the modern submarine massive sulfide deposits in hydrothermal ore areas of the Eastern Pacific Rise (occurrence 6° N and massive sulfide deposits in the range of 18°5' to 21°8' S) and two hydrothermal fields of Mid Atlantic Ridge (active section Irina-2 14°5' N in Logachev field and Rainbow field 36°14' N). Probable causes of these variations are discussed.

7 figures, 1 table, 10 references.

Keywords: hydrothermal ores at the oceanic bottom, sulfide-oxide mineral assemblages, sulfur and oxygen regime during modern submarine ore-formation.

According to the study of continental deposits, S and O regimes are important for ore-formation and depend on geological and physicochemical factors. These regimes are opposite that is exhibited with juxtaposition of different stages or with facial changes of mineral assemblages during a single stage. As illustrated by the Fe-S-O and Fe-Cu-S-O systems (Betekhtin, 1953), the "fight" between sulfur and oxygen regimes determines many common features in mineral assemblages and distribution of metals at deposits.

Let us discuss this problem as applied to the modern submarine hydrothermal ores. By the elements of variable valence, the major minerals of oceanic massive sulfide deposits are extremely sensitive to the change of geochemical parameters. Four hydrothermal ore areas in different geodynamic environment were selected to be investigated:

- occurrence 6° N, Eastern Pacific Rise (EPR);
- hydrothermal complex of massive sulfide deposits in the range of 18°5' to 21°8' S, EPR;
- active location Irina-2 14°5' N, Logachev field, Mid Atlantic Ridge (MAR);
- Rainbow field 36°4' MAR.

Major ore minerals in the sulfide-oxide assemblages are pyrrhotite $Fe_{1-x}S$, pyrite FeS_2 ,

marcasite FeS_2 , chalcopyrite $CuFeS_2$, isocubanite $CuFe_2S_3$, bornite Cu_5FeS_4 , chalcocite Cu_2S , sphalerite $(Zn,Fe)S$, and hematite Fe_2O_3 .

Brief description of selected areas

Occurrence 6° N, EPR was discovered in 1990 in the northern near-equatorial zone of EPR during Cruise 9 the R/V *Geologist Fersman*. Significantly eroded flattened and isometric sulfide mounds are at the western flank of axial graben. They are located on the even surface of basalt flow and slightly covered by sediments. The largest mounds are 0.8 m in diameter and height. Total weight of collected sulfides was 112 kg. According to structural and mineralogical features, the following major varieties of sulfide ore are distinguished: zoned fragments of chimneys, complex breccia ore, and porous ore. Pyrite, chalcopyrite-pyrite, and sphalerite-pyrite-marcasite assemblages with abundant shells of vestimentifera were identified in the latter. Coloform and/or gel sulfides are widespread.

Massive sulfide hydrothermal complex (18°5' 21°8' S, EPR) occurs on the basalt flow (Tufar, 1993). Groups of black smokers up to few meters high are characteristic. Like

occurrence 6° N, numerous inclusions of vestimentifera relicts were identified in the fragments of black smokers. Iron, copper, and zinc sulfides are the major ore minerals. Coloform segregations of sulfides are intergrown frequently with high-temperature sulfides (for example, isocubanite and chalcopyrite) indicating disequilibrium conditions of mineralization (Tufar, 1993).

Section Irina-2 located within the Logatchev hydrothermal field was discovered during Cruise 7 (1993–1994) of the R/V *Professor Logatchev* and was studied by many researchers with both shipborne devices and submersible. This field located at the junction zone of small rift step and large step at a depth of 2970–3000 m. The step is a top surface of ridging serpentinite massif. This structure is confined to the large zone of transverse tectonic dislocations. More than 10 ore hills (the largest one is 200×100 m) were found within the field. Main part of the field is inactive. The active areas are located in linear structure passing through its center from NW to SE (Mozgova *et al.*, 1999).

As a result of the detailed study of the hydrothermal field with the submersible, separate active locations were marked. For example, in 1995, as a result of four submerges of submersible from French R/V *Nadir* locations Irina-1 and Irina-2 were found; these locations were named in honor of I.M. Poroshina, a researcher of All-Russia Research Institute for Geology and Mineral Resources of the World Ocean, who participated in the cruise. The samples studied here were collected from the Irina-2 active chimney complex in 2001 during cruise of R/V *Atlantis* with the *Alvin* submersible.

Like the Logatchev field, the **Rainbow hydrothermal field** (36°4' N, MAR) related to ultramafic rocks was discovered in 1997 (Fouquet *et al.*, 1997). This field located at a depth of 2270–2329 m is confined to the western slope of axial rise of the MAR rift composed of serpentinite. The field extends in latitudinal direction for 250 m with 60 m wide. Numerous active and varied relict sulfide mounds were found within it: single chimneys of 2–3 m to few cm high, groups of intergrown chimneys, mounds composed of large fragments of massive sulfides, and hills consisting of their oxidizing products. The

detailed study of young zoned active chimneys (samples were collected during Cruise 47 of the R/V *Academician Mstislav Keldysh* in 2002) allowed us to discuss of mechanism of their formation and to develop the known models of formation of sulfide chimneys of black smokers (Borodaev *et al.*, 2004). This article is focused only relationship between sulfide and oxide paragenetic assemblages.

Description of sulfide–oxide mineral assemblages studied

As aforementioned, three major varieties of porous sulfide ore are distinguished in picked up material from the occurrence of near-equatorial part of EPR (6° N): pyrite, chalcopyrite-pyrite, and sphalerite-pyrite-marcasite. In places, they are overprinted by magnetite-hematite assemblage. The samples, where hematite, magnetite and pyrite are the major minerals, are the most attractive. Microscopically, these minerals display frequently controversial relationship. Small polished banded ore sample of 2×2 cm in size (Fig. 1), in which oxides concentrate in darker bands, whereas light bands consist mainly of pyrite with the lightest and coarse-grained zone (Fig. 1, bottom) composed of its branching intergrowths, exemplifies this. As a result of detailed microscopic study in reflected light, variable relationships of these minerals were revealed.

The replacement of hematite crystals by magnetite up to complete pseudomorphs as a result mushketovite formation is the earliest (Fig. 2a). Microcoloform aggregates of pyrite occur as veinlets (Fig. 2b) or areas (Fig. 2c) after these pseudomorphs. Hereafter, small crystals of hematite-II overgrow both magnetite pseudomorphs (Fig. 3a) and branching aggregates of pyrite from the outer part of the sample (Fig. 3b). At the same time, coloform zoned pyrite with separate small inclusions of hematite along boundaries between zones is observable (Fig. 3c). Shape of these inclusions is governed by the morphology of boundaries of coloform zones allowing attribution this hematite also to the second generation. Hematite crystals with inclusions of pyrite fragments among pyrite breccia exemplify hematite later than pyrite (Fig. 3d).

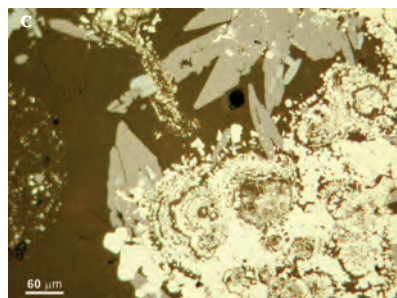
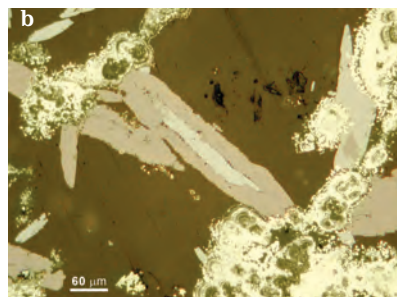
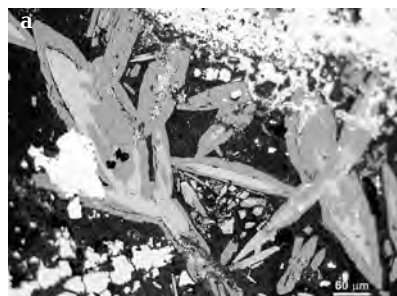
It is apparent that the data obtained testify to oscillation and facial variability of oxide-



Fig. 1. Polished ore specimen with banded (zoned) structure from submarine massive sulfides (6° N, EPR). Oxides concentrate in the darker zone, pyrite is in the lighter zones, and branching intergrowths of pyrite occur in the lower marginal coarse-grained zone. Size of the specimen is 2×2 cm. Photo in reflected light.

Fig. 2. Relationship of hematite, magnetite, and pyrite in the dark ore zone shown in Fig. 1. Polished sections. Photo in reflected light. Hematite crystals are light grey; magnetite is dark grey; and pyrite is white:

a – pseudomorphs of magnetite after hematite (mushketovization); b, c – microcolloform segregations of pyrite: cutting (b) and replacing (c) pseudomorphs of magnetite.



sulfide conditions with microspace and time during the formation of submarine massive sulfides in the near-equatorial areas of EPR.

Mineralogy of massive sulfides in the range of 18°5'–21°8' S of EPR studied in detail by Tufar (1993) is similar to that reported in the northern part of the same rise. According to Tufar (1993), hematite occurred as aggregates of euhedral crystals intergrown with chalcopyrite, pyrite, melnikovite-pyrite, marcasite, and isocubanite (Tufar uses outdated name chalcopyrrhotite) is abundant in some fragments of black smokers and zone enriched in copper. Together with pyrite and melnikovite-pyrite, hematite is present in rhythmic concentric-colloform layered crusts and colloidal masses.

Despite the absence of special discussion concerning age relationship between hematite and sulfide in the cited paper, the description of assemblage of the mineral and won-

derful illustrations given in it suggest that sulfide-oxide relationship in the southern massive sulfide complex (18°5'–21°8' S, EPR) are similar to those described from near-equatorial areas of EPR (6° N). In the southern complex, the quantitative relationship of oxides and sulfides is highly variable. Hematite corrodes and overgrows relicts of sulfide minerals (pyrite, chalcopyrite), contains fragments of pyrite, and in some zones is replaced by magnetite occasionally up to complete pseudomorphs like the northern occurrence of EPR. Small rounded flakes and clusters of small crystals of later hematite overgrow large hematite crystals in numerous cavities in pyrite-hematite ore.

Thus, in spite of long distance between these two massive sulfide complexes in EPR, they are characterized by similar mineral assemblages indicating similar variations in sulfur and oxygen regime.

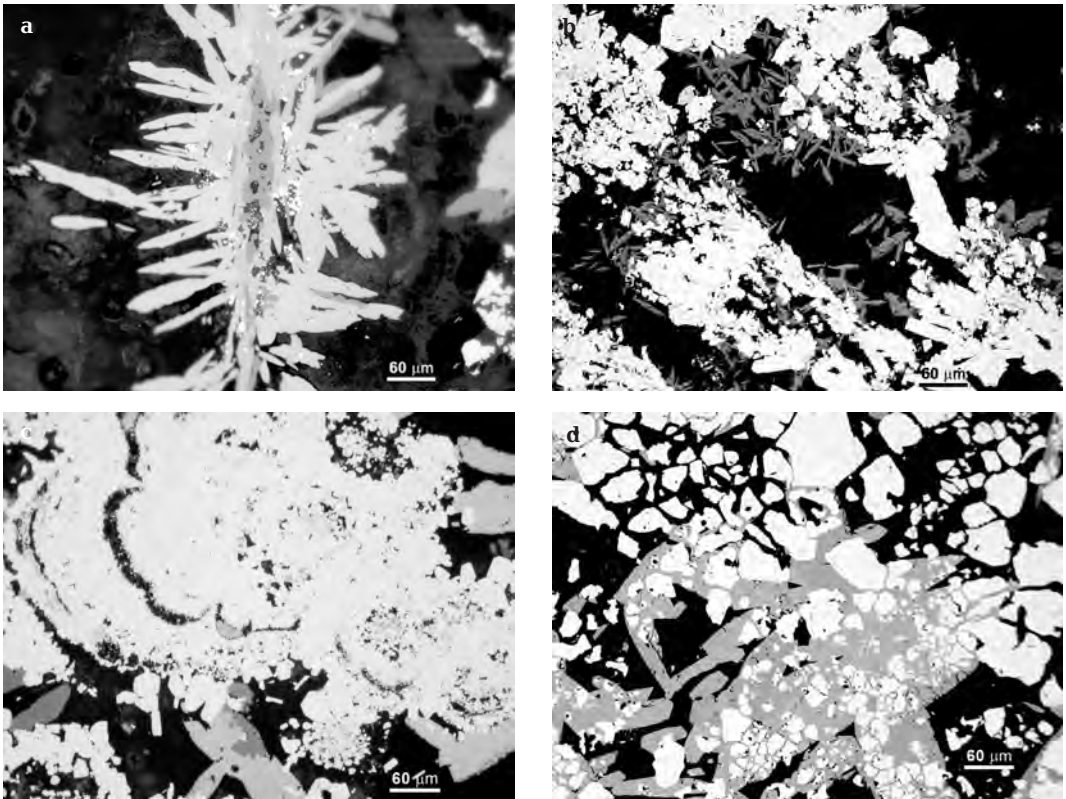


Fig. 3. Relationship between hematite-II and relicts of magnetite pseudomorphs after early hematite and aggregates of pyrite in submarine massive sulfides (6°N, EPR). Polished sections. Photo in reflected light:

a – small crystals of hematite on magnetite (grey) pseudomorph after early hematite; b – aggregate of pyrite grains overgrown by crystals of hematite-II; c – small inclusions of hematite on the boundaries of zones in colloform pyrite; these inclusions are governed by zone boundaries; d – crystals of hematite with inclusions of pyrite fragments enclosed in pyrite breccia.

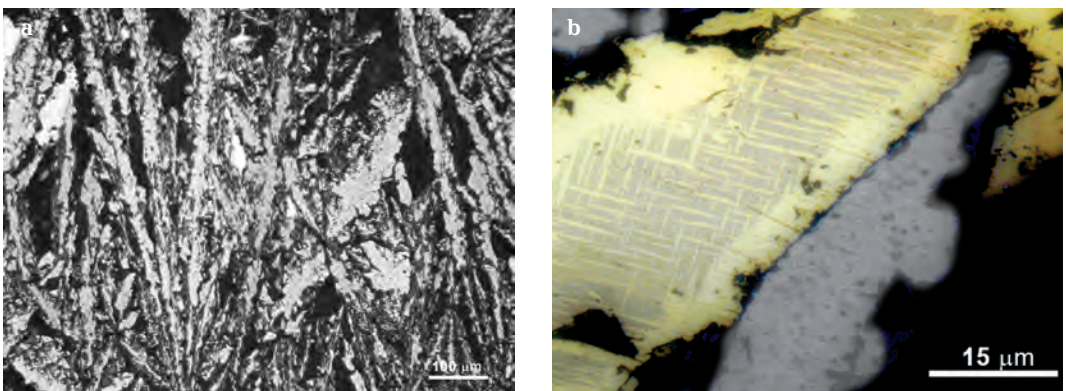


Fig. 4. The first type of relationships between sulfides and oxides at the Irina-2 location, Logatchev field, MAR. Polished sections. Photo in reflected light:

a – radiated aggregate of hematite with single small lance-shaped grains of isocubanite between elongate hematite crystals; b – detail; structure of separate lense (upper left) in hematite aggregate: lattice texture of exsolved isocubanite – blades of chalcopyrite (light yellow) in isocubanite matrix (light grey) rimmed by chalcopyrite.

In the ore samples of the Irina-2 active location, Logatchev field, MAR, we have found: hematite, bornite, chalcocite, and iron hydroxides. Three types of relationships were revealed between them.

Relationship between hematite and isocubanite and chalcopyrite is attributed to the first type. Fine isolated lenses of exsolved isocubanite fill interstices between coarse-grained radiated hematite (Fig. 4a). Cores of the lenses are lattice exsolution texture (Fig. 4b), where lattice formed by fine blades is in the cubanite matrix and whole lattice aggregate is rimmed by chalcopyrite. It should be emphasized that the shape of lenses and chalcopyrite rims are subject to morphology of hematite aggregates. It suggests that high-temperature ($T > 300^\circ$) homogeneous isocubanite (or chalcopyrite) solid solution enriched in copper crystallized initially, then this solid solution was exsolved to liberate copper as chalcopyrite blades and rims.

The second-type relationships are between hematite and chalcopyrite, bornite, and chalcocite (Fig. 5). Microscopically in reflected light, veinlets of chalcopyrite cut and corrode hematite and contain its relicts (Fig. 5a). At the same time, a narrow zone of bornite with relict chalcopyrite occurs after chalcopyrite close to contact with hematite. Chalcocite rim is seen occasionally immediately at the contact with hematite (Fig. 5b). Bornite develops in place after chalcopyrite that corroded and replaced hematite in outer part of its radiated aggregates. Small irregular-shaped relicts of chalcopyrite and chalcocite strings on the continuation of hematite rays are observed in bornite (Fig. 5c). In these cases, it is evident that bornite and chalcocite in chalcopyrite close to hematite are resulted from oxygen released from the hematite replaced.

The third-type relationships are characteristic of the iron oxides and hydroxides + chalcopyrite + bornite + chalcocite assemblage (Fig. 6). In these assemblages, relicts of hematite are replaced by iron hydroxides¹ nearly to complete pseudomorphs with reddish inner reflections (Fig. 6a).

Zoning described in the second-type relationships is occasional around large pseudo-

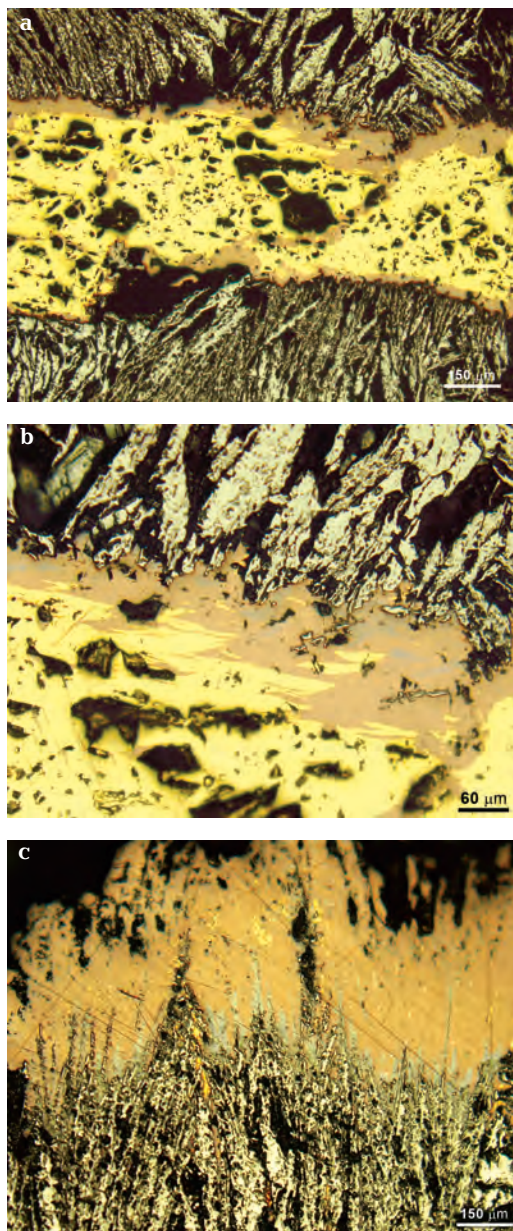


Fig. 5. The second type of relationships between ore minerals at the Irina-2 location. Reaction transformation at the contact between coarse-radiated hematite and cut veinlet of chalcopyrite. Polished sections. Photo in reflected light: a – general view of chalcopyrite veinlet cutting hematite with reaction rim of bornite (brown) at contacts; b – near-contact area with remarkable bluish grey spots of copper sulfide (chalcocite) at high magnification; c – metasomatic bornite zone (light brown) after chalcopyrite at the outer part of radiated aggregates of hematite; bornite contains small relicts of chalcopyrite and string-shaped chalcocite segregations (bluish green) on the continuation of hematite rays.

¹ – Exact identification of the minerals is impossible because of fine-grained texture and microheterogeneity of the pseudomorphs.

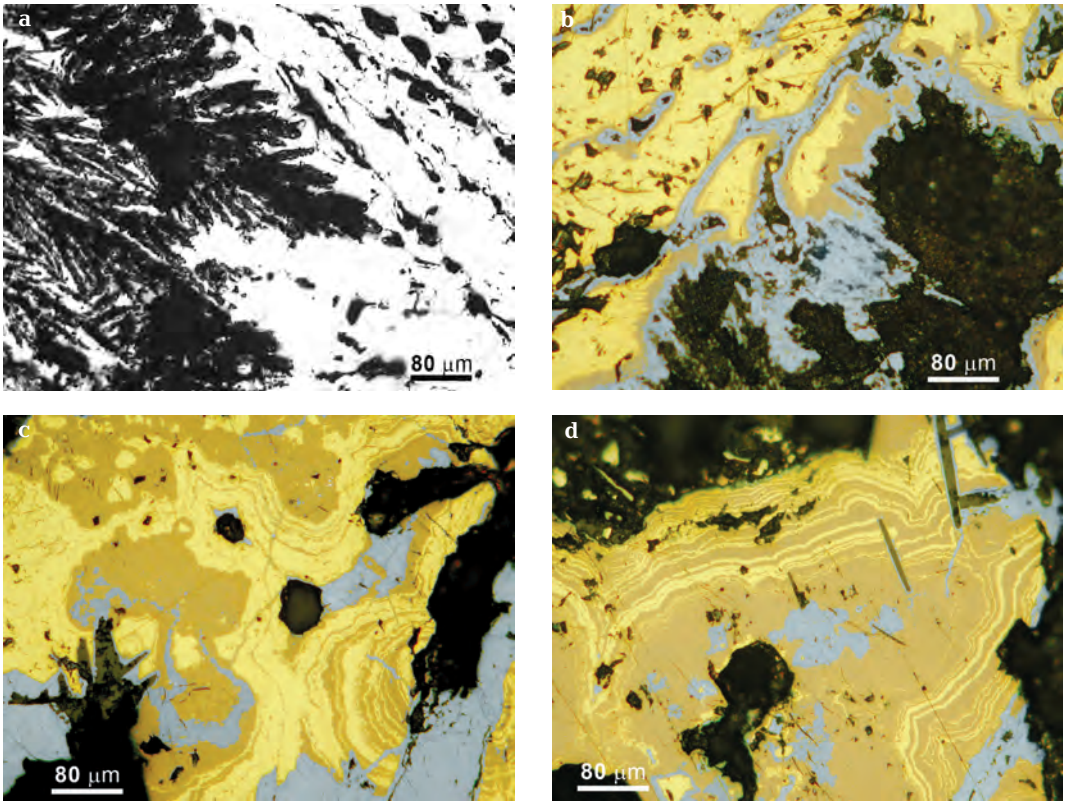


Fig. 6. The third type of relationships between iron hydroxides, chalcopyrite, bornite, and chalcocite, Irina-2 location. Polished sections. Photo in reflected light:
 a – complete pseudomorph of iron hydroxides (black) after branching hematite segregation enclosed in pyrite (white);
 b – two reaction metasomatic zones, chalcocite (bluish green) and bornite (brownish) alternating each other from pseudomorph of iron hydroxides after hematite to hosting chalcopyrite (yellow); the same zoning exhibits in thin veinlets cutting chalcopyrite;
 c, d – chalcopyrite-bornite coloform-zoned aggregates with inclusions of relicts of iron hydroxide pseudomorph after hematite; the character of intergrowths and relation of component are variable.

morphs (Fig. 6b): chalcocite zone adjacent to pseudomorph is followed by zone of bornite that contacts with relicts of chalcopyrite replaced. Alongside, chalcopyrite is cut by net of thin symmetrically zoned veinlets, where similar sequence of thin zones is observable: bornite zone extended along contact with chalcopyrite is followed by chalcocite zone toward central part of veinlet and discontinuous very thin black band (probably, cavities with iron hydroxides) is in the central part immediately. In the other adjacent places (Figs. 6c, 6d), zoned coloform bornite-chalcopyrite aggregates with variable width of zones and quantitative relationship of bornite and chalcopyrite are abundant. Relicts of pseudomorphs of iron hydroxides after hematite are observed also in them, but

zoning shown in Fig. 6b is absent. Therein, chalcocite occurs mainly as spots and veinlets.

In the Rainbow hydrothermal field (36°4' N, MAR), different authors have reported more than 30 minerals including native metals, sulfides, sulfates, oxides, hydroxides, and carbonates. Therein, relationships differ from described above (Fig. 7). On the one hand, these are interaction of iron hydroxides with high-temperature assemblage consisting of pyrrhotite, sphalerite, and isocubanite, on the other hand, these are relationships between iron hydroxides and lower-temperature assemblage of coloform aggregates composed of pyrite, marcasite, and sphalerite. In the former case, iron hydroxides replace intensively lamellar crystals of pyrrhotite nearly up to

complete pseudomorphs. Relicts of pyrrhotite crystals are included occasionally into sphalerite-isocubanite aggregate and then, iron hydroxides rim the whole aggregate (Fig. 7a). In the other places, the hydroxides replace nearly completely fine-acicular part at the bottom of radiated aggregate of tabular pyrrhotite crystals and occur as crust on this aggregate on the side of fresh tabular crystals (Figs. 7b, 7c). According to chemical data (Table), relict of lamellar pyrrhotite contains more Fe ($x = 0.06$ in formula $Fe_{1-x}S$), than tabular pyrrhotite in radiated aggregate ($x = 0.12$). As is known, symmetry of the pyrrhotite lattice depends of deficiency of Fe and at $x \sim 0.11$ to 0.20 , hexagonal pyrrhotite transforms

to monoclinic (Minerals..., 1960). Based on these data, the early relict of pyrrhotite (Fig. 7a) may be considered as hexagonal and pyrrhotite in radiated aggregate (Fig. 7b), as monoclinic.

In the lowest-temperature assemblage composed of coloform grains, pyrite is in the cores of these grains and columnar radiated marcasite, in margins (Fig. 7c). These aggregates are surrounded by zoned rim with discontinuous chains of small crystal of Fe-rich sphalerite enclosed in thin zones of iron hydroxides with bright red inner reflections. The chemical composition of sulfide minerals is given in the Table. In similar rims, separate inclusions of small barite crystals close to

Fig. 7. Relationships between pyrite, sphalerite, and isocubanite and iron hydroxides, Rainbow field, MAR. Polished sections. Back-scattered electron images:

- a – tabular crystal of pyrrhotite is replaced by iron hydroxides to form pseudomorph. The crystal is surrounded by sphalerite (light grey) with crenate segregation of isocubanite (slightly darker). All aggregate is rimmed by columnar hydroxides;
- b – radiated aggregate of tabular pyrrhotite crystals transiting to fine-acicular segregation that is nearly completely replaced by iron hydroxides. Another side of fresh crystals of pyrrhotite is rimmed by iron hydroxides;
- c – coloform pyrite-marcasite aggregate (pyrite in the center; columnar radiated marcasite in margins) is rimmed by discontinuous chain of fine crystals of Fe-rich sphalerite (white) surrounded by thin zones of iron hydroxides with bright red inner reflections;
- d – detail of (c).

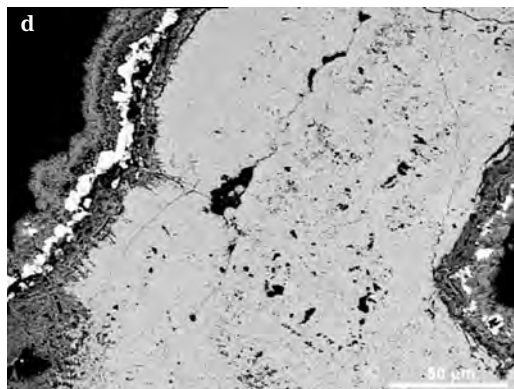
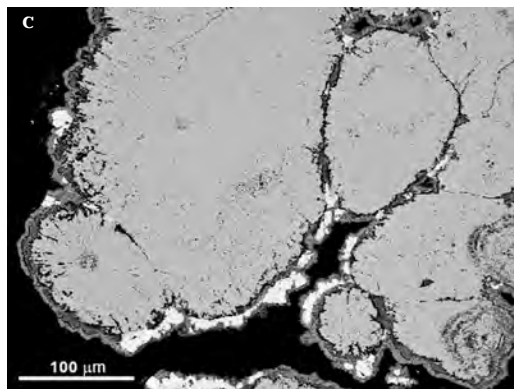
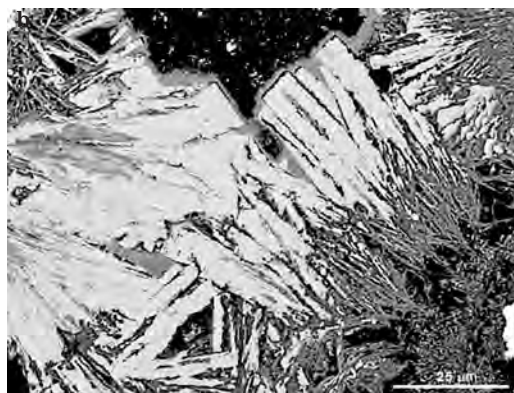
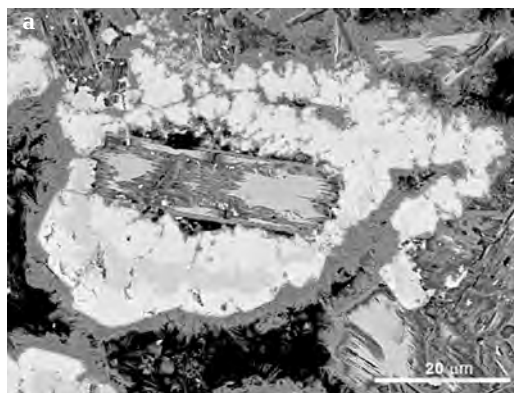


Table 1. Electron microprobe data of sulfide minerals from submarine massive sulfides of the Rainbow, wt.%

Mineral	Fe	Cu	Zn	Co	S	Total	Formula	Figure
Pyrrhotite	60.83	—	—	—	37.30	98.13	Fe _{0.94} S	7a
— " —	59.69	—	—	0.21	38.77	98.67	Fe _{0.88} S	7b
— " —	60.56	0.64	—	—	39.53	100.73	Fe _{0.88} S	7b
Pyrite	46.71	—	—	—	53.14	99.85	Fe _{1.01} S _{1.99}	7c, d
Marcasite	45.92	—	—	—	54.54	100.46	Fe _{0.98} S _{2.02}	7c, d
Sphalerite	21.96	0.07	42.27	—	34.21	98.51	(Zn _{0.62} Fe _{0.37}) _{0.99} S _{1.01}	7c, d
— " —	23.75	0.17	41.28	—	35.20	100.40	(Zn _{0.58} Fe _{0.39}) _{0.98} S _{1.02}	7c, d

Notes. Formula of pyrrhotite is calculated on the basis of 1 atom S; formula of pyrite and marcasite, on the basis of 3 atoms per formula; and formula of sphalerite, on the basis of 2 atoms per formula.

sphalerite chains and growth direction of zones of columnar hydroxides are seen at high magnification; these zones grow from central chains of sphalerite crystals both outward and to marcasite replacing it (Fig. 7d).

Thus, on the one hand, iron hydroxides replace sulfides; on the other hand, they cover them by thin crusts containing interlayers of newly formed sulfides.

Discussion

Mineral assemblages of iron sulfides and oxides are abundant in varied types of continental deposits. Betekhtin (1953) discussed numerous examples of these assemblages with emphasis on change of mineral assemblages testifying to change of sulfur and oxygen regime during deposition.

We have studied this problem with application to modern sulfide-oxide mineral assemblages in massive sulfides for the last decade; some our results were reported at the international mineralogical conferences (Mozgova *et al.*, 2004₁; 2004₂). The aforementioned data indicate that the assemblages studied in submarine massive sulfides are variable in both quantitative and age relationships of sulfide and oxide constituents, which frequently change in microspace and time. Therefore, they reflect corresponding change of sulfur and oxygen regime and suggest causes of such changes. Microscopic observations in reflected light are important for such studies. We dwell on two most dramatic examples from described above.

One of them is relationships in sulfide-oxide assemblages in massive sulfide samples from occurrence 6° N, EPR. Microscopically,

in places, where mineralogy of ore is relatively simple (ore assemblage consists of hematite of different generations, magnetite, and pyrite), clear sequence of mineral formation indicating change of sulfur and oxygen fluid regime is observed. Initially formed hematite lamellas (mineral with the highest oxidation level) are mushketovitized, i.e., are replaced by magnetite (the mineral depleted in oxygen). The process starts from the formation of rims and finishes by the formation of complete pseudomorphs (Fig. 2). At the same time, colloform zoned aggregates of pyrite are formed. These relationships correspond to known reaction of mushketovitization under effect of H₂S that is strong reducing agent: 2Fe₂O₃ + 2H₂S = Fe₃O₄ + FeS₂ + H₂O (Betekhtin, 1953). Hereafter, the inverse process occurs: both relicts of magnetite pseudomorphs and accompanying pyrite are overgrown by small euhedral hematite-II crystals. On the one hand, this may indicate to the change of sulfur and oxygen regime determining the damping of sulfide deposition and, on the other hand, to introducing new portions of sea water, that according to some studies (for example, Constantinou, 1975) is good oxidizing agent. For example, according to the same author, pyrite converses to goethite even at the lowest concentration of oxygen in sea water (0.1 ml per liter).

Ore assemblages of the Irina-2 active location, Logatchev field, MAR provide another example. Therein, early coarse-grained radiated hematite with rare small inclusions of exsolved high-temperature (> 300°C) isocubanite has been described. It appears to testify to nearly simultaneous precipitation of hematite and high-temperature isocubanite

solid solution during its homogeneous stage (Fig. 4). In another sample, veinlet of chalcopyrite cuts and corrodes similar hematite (Fig. 5). Along margins of the veinlet, reaction rim of bornite, copper sulfide depleted in Fe in comparison with chalcopyrite and containing Fe-free chalcocite, is formed at the contact with hematite. It is obvious that the transformation is due to oxygen released as a result of replacement of hematite. Under these conditions, iron from near-contact chalcopyrite removes and chalcopyrite close to the boundary with hematite converses to bornite initially and then, to chalcocite. The similar removal of iron from chalcopyrite to form reaction rims under oxidative conditions was described multiple at the continental deposits. For example, in massive sulfides of Cyprus, as a result of oxidative leaching of chalcopyrite, the formation of reaction zones of Cu-rich idaitite (Cu_3FeS_4) is followed by precipitation of covellite (CuS) (Constantinou, 1975). Betekhtin described removal of iron from chalcopyrite under oxidative conditions, similar to those, which we reported, to form reaction rims of bornite and chalcocite. This phenomenon is caused by capacity of iron to release from chalcopyrite, "whereas copper having high affinity to sulfur can be preserved as sulfides depleted in Fe or Fe-free under the same conditions" (Betekhtin, 1953).

Thereafter, in submarine massive sulfides, hematite aggregates are replaced by amorphous iron hydrosulfides up to complete pseudomorphs (Fig. 6). Relicts of such pseudomorphs surround chalcopyrite and chalcopyrite-bornite color zoned aggregates. This process is accompanied in places by strong releasing iron not only from chalcopyrite but bornite also that results in the formation of thin zone of chalcocite immediately at the contact with relicts of hydroxide pseudomorphs after hematite; this zone replaces bornite that in turn develops after chalcopyrite (Fig. 6b).

Restricted by these examples, it can be concluded that sulfur and oxygen regime is widely variable in the modern submarine massive sulfides like continental hydrothermal deposits. It is reflected in change of iron sulfide and oxide assemblages. As hydrothermal process dies out, mineral assemblages change to lower-temperature depleted in sul-

fide sulfur (up to its complete disappearance) ones. At the same time, in accordance with varied state of fluids or oxidizing capacity of replaced minerals, relationships of sulfide-oxide mineral assemblages may alternate in microspace and time during mineralizing process. It is consistent with thermochemical theoretical calculations, according to which, iron oxides converse to sulfides and reverse within narrow range of pH and Eh (Garrels and Christ, 1965). The results obtained support the conclusion by Betekhtin that this regime multiple alternates during ore deposition including microscale.

Acknowledgements

We thank S.N. Nenasheva and E.A. Borisova, Fersman Mineralogical Museum, Russian Academy of Sciences, for discussion and helpful advices.

References

- Betekhtin A.G.* Hydrothermal solutions, their nature and ore-formation process // The main problems in the study of magmatogenic ore deposits. Izd. AN SSSR, Moscow. **1953**. P. 122–275. (in Russian).
- Borodaev Yu.S., Mozgova N.N., Gablina I.F., Bogdanov Yu.A., Starostin V.I., Fardust F.* Zoned chimneys of black smokers from the Rainbow hydrothermal field, Mid Atlantic Ridge 34°14' N. // Vestnik Moscow Univ. Ser. Geol. **2004**. No 3. P. 35–48. (in Russian).
- Constantinou G.* Idaitite from the Skoriotissa massive sulfide orebody, Cyprus: its composition and conditions of formation. *Amer. Mineralogist*. V. 60. **1975**. P. 1013–1018.
- Fouquet Y.Y., Charlou J.-L., Ondreas H. et al.* Discovery and first submersible investigations on the Rainbow hydrothermal field on the MAR (36°14' N). *EOS Amer. Geophys. Union. Transactions*. V. 78(46). **1997**. P. 832.
- Garrels R.M. and Christ C.L.* Solutions, minerals, and equilibria. Harper & Row, New York. **1965**.
- Minerals. Handbook*. V. 1. Izd. AN SSSR, Moscow. **1960**. (in Russian).
- Mozgova N.N., Efimov A.V., Borodaev Yu.S. et al.* Mineralogy and chemistry of massive

sulfides from the Logatchev hydrothermal field (14°45' N Mid-Atlantic Ridge). *Explor. Mining Geol.* **1999**. P. 8 (3–4), 379–395.

Mozgova N., Cherkashev G., Borodaev Yu., Stepanova T., Zhirnov E., and Uspenskaya T. Sulfur and oxygen regimes in modern submarine hydrothermal ore-formation. 32nd IGC Florence 2004-Scientific sessions: Abstracts (part 2). Florence. **2004**₁. P. 1197.

Mozgova N., Cherkashev G., Borodaev Yu., Stepanova T., Zhirnov E., Uspenskaya T., Bern-

hardt H.-Yu. Oxide-sulfide assemblages as an indicator of sulfur and oxygen regimes in modern submarine hydrothermal sulfide formation. *Minerals of the Ocean. Integrated strategies-2*. International conference. 25–30 April, 2004. Abstract. St. Petersburg: VNIIOkeangeologia. **2004**₂. P. 163–164.

Tufar W. Recent complex massive sulfides mineralizations (black smokers) from the Southern part of the East Pacific Rise. *Arch. f. Lagerst. forsch. Geol. B.-A. Wien.* **1993**. B. 16. P. 109–145.